

Enzymatic Degradation and Adsorption on Poly[(*R*)-3-hydroxybutyrate] Single Crystals with Two Types of Extracellular PHB Depolymerases from *Comamonas acidovorans* YM1609 and *Alcaligenes faecalis* T1

Tadahisa Iwata and Yoshiharu Doi*

Polymer Chemistry Laboratory, The Institute of Physical and Chemical Research (RIKEN), Hirosawa, Wako-shi, Saitama 351-01, Japan

Takao Tanaka and Takashi Akehata

Faculty of Engineering, Science University of Tokyo, 1-3 Kagurazaka, Shinjuku-ku, Tokyo 162, Japan

Masakatsu Shiromo and Shinya Teramachi

Department of Applied Chemistry, Kogakuin University, Hachioji, Tokyo 192, Japan

Received April 10, 1997; Revised Manuscript Received July 3, 1997[®]

ABSTRACT: Poly[(*R*)-3-hydroxybutyrate] (P(3HB)) single crystals, which had different morphologies with and without chain-folding surfaces, were grown from dilute solutions of chloroform and ethanol. Two types of extracellular PHB depolymerases purified from *Alcaligenes faecalis* T1 and *Comamonas acidovorans* YM1609, defined as types I and II according to the position of the lipase box in the catalytic domain, were used in the enzymatic degradation and adsorption experiments. The enzymatic degradation of P(3HB) single crystals was investigated by means of transmission electron microscopy, atomic force microscopy, and gel-permeation chromatography. Adsorption of PHB depolymerase on P(3HB) single crystals was examined using an immuno-gold labeling technique. Enzymatic degradation of single crystals progressed from the edges and ends of crystals to yield the narrow cracks and the small crystal fragments along their long axis, independent of both surface morphologies of single crystals and types of extracellular PHB depolymerases. Lamellar thicknesses of single crystals and molecular weights of P(3HB) chains remained unchanged during the enzymatic hydrolysis. Adsorption of extracellular PHB depolymerase demonstrated a homogeneous distribution of enzyme molecules on the chain-folding surface of crystals. The above results suggest that the adsorption of enzyme increases with the mobility of P(3HB) chains of single crystals as a whole and that the *endo*–*exo* type attack by the active-site of PHB depolymerase takes place preferentially at the disordered chain-packing regions of crystal edges and ends rather than the chain-folding surfaces of single crystals, in spite of the difference in the structure of enzymes.

Introduction

Poly[(*R*)-3-hydroxybutyrate] (P(3HB)), which is produced by a wide variety of bacteria,^{1,2} is a biodegradable thermoplastic. The biodegradability of P(3HB) has been evaluated in various environments such as in soil, sludge or sea water.³ Until now, several extracellular PHB depolymerases have been purified from bacteria such as *Pseudomonas lemoignei*,⁴ *Alcaligenes faecalis*,⁵ *Comamonas testosteroni*,⁶ *Pseudomonas stutzeri*,⁷ *Pseudomonas pickettii*⁸ and *Comamonas acidovorans*.⁹ The characterizations of the structural genes revealed that PHB depolymerases were organized with catalytic, linker, and substrate-binding domains.^{9–11} Such structures have also been already reported in other microbial enzymes which depolymerize water-insoluble polymer materials such as cellulase,¹² xylanase,^{12–14} chitinase,^{15,16} and arabinofuranosidase.¹⁴

Recently, extracellular PHB depolymerases were classified into three types (types I, II and III) by differences in the linker–domain structure or in the position of lipase box in the catalytic domain.^{17,18} Type I enzymes are represented by *P. lemoignei* PhaZ4 (isoenzyme PHV depolymerase 1)¹⁹ and *A. faecalis* T1,²⁰ while type II enzymes are produced by *Comamonas* sp.,¹⁷ *Streptomyces exfoliatus*¹⁸ and *C. acidovorans* YM1609.⁹ As shown

in Figure 1, both types I and II have a fibronectin type III module fingerprint (Fn3) as the linker-domain, whereas the linker-domain of type III enzyme as represented by *P. lemoignei* PhaZ5 (isoenzyme A),¹⁹ consists of threonine-rich region. Types I and II are distinguished by the position of the lipase box in the catalytic domain; the lipase box in type I is located around the center of the catalytic domain, while the lipase box in type II exists near the N-terminal. However, there is little information on the relation between the structure of PHB depolymerase and the behavior of enzymatic hydrolysis.

Enzymatic hydrolysis of P(3HB) and its copolymers have been extensively studied on solution-cast films²¹ and melt-crystallized films,^{22–24} which demonstrated that the enzymatic hydrolysis occurred first at the amorphous region and subsequently at the crystal region. To elucidate the mechanism of enzymatic degradation on the crystal region, single crystals were prepared as the model substrate, and their enzymatic degradation was studied. For example, enzymatic degradation using single crystals was performed on β -(1 \rightarrow 4)xylan single crystals with xylanases²⁵ and lamellar single crystals of nigeran with mycodextranase.²⁶ Recently, these techniques were applied to P(3HB) single crystals.

The enzymatic degradation of P(3HB) single crystals was first studied by Hocking *et al.*,^{27,28} using two types of PHB depolymerases from the fungus *Aspergillus*

* To whom all correspondence should be addressed. Phone: +81-48-467-9402. Fax: +81-48-462-4667.

© Abstract published in *Advance ACS Abstracts*, August 15, 1997.

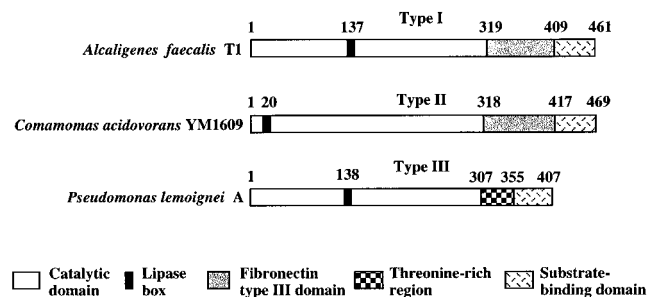


Figure 1. Domain structures of extracellular PHB depolymerases purified from *A. faecalis* T1,⁵ *C. acidovorans* YM1609⁹ and *P. lemoignei* A.¹⁹

fumigatus and the bacterium *P. lemoignei*. From the results of both turbidimetric and titrimetric assays and of molecular weight measurement, they concluded that the enzymatic degradation occurred from the crystal edges rather than the chain folds of the lamellar surfaces and supported the hypothesis of combined *endo-exo* degradation. Nobes *et al.*²⁹ have recently found the splintering of P(3HB) single crystals during the course of enzymatic degradation by an extracellular PHB depolymerase A from *P. lemoignei*, using the transmission electron microscopy, and concluded that the enzyme has both *endo* and *exo* activities.

On the other hand, in a previous paper³⁰ we studied the enzymatic degradation of P(3HB) single crystals with an extracellular PHB depolymerase purified from *Pseudomonas stutzeri* YM1006, using transmission electron microscopy, atomic force microscopy and gel permeation chromatography, together with the study on the adsorption of enzyme by an immuno-gold labeling technique. On the basis of these observations, we concluded that hydrolysis by the active-site of PHB depolymerase takes place preferentially at the disordered chain-packing regions of crystal edges rather than the chain-folding surfaces of single crystals, in spite of the unselective adsorption of enzyme, and that untied or exposed P(3HB) chains are degraded predominantly by the *exo-type* behavior of enzyme.

In this paper, we have attempted to obtain more insight on the mechanism of the hydrolysis of P(3HB) single crystals by two different types of extracellular PHB depolymerases purified from *A. faecalis* T1 and *C. acidovorans* YM1609, defined as types I and II as shown in Figure 1, using transmission electron microscopy, atomic force microscopy and gel-permeation chromatography. These results are compared with those reported for the type III PHB depolymerase, *P. lemoignei* PHB depolymerase A.²⁹ Immuno-gold labeling technique was also adopted to visualize the adsorption of enzyme to single crystals.

Experimental Section

P(3HB) Samples. Two kinds of P(3HB) samples with different molecular weights were prepared from the bacterial P(3HB) (number-average molecular weight (M_n) = 358 000 and polydispersity (DPI) = 2.8), purchased from Aldrich Chemical Co., Ltd., by aqueous KOH alkali-hydrolysis with 18-crown-6 ether according to the method described previously.³⁰ One is LMW-P(3HB) which has M_n = 1700 and DPI = 1.2, and the other is HMW-P(3HB) which has M_n = 34 000 and DPI = 2.6.

Preparation of Single Crystals. Single crystals of both P(3HB) samples were prepared from dilute solution according to a method derived from that of Marchessault *et al.*³¹ P(3HB) samples were dissolved into chloroform and recrystallized by the addition of an excess of ethanol. Their preparation and base plane electron diffractogram were described previously.³⁰ The crystals were collected by centrifugation and washed three times with room temperature ethanol. For enzymatic degra-

dation and adsorption experiments, the crystals were collected by centrifugation, washed with 50 mM Tris-HCl buffer, and resuspended in the same buffer.

Enzymatic Degradation of Single Crystals. The extracellular PHB depolymerases from *C. acidovorans* YM1609 and *A. faecalis* T1 were purified to electrophoretic homogeneity by the methods of Kasuya *et al.*⁹ and Tanio *et al.*⁵ respectively. Degradation of P(3HB) single crystals was monitored using a turbidimetric assay. 4 μ L of a 200 μ g/mL solution of an extracellular PHB depolymerase purified from *C. acidovorans* YM1609 or *A. faecalis* T1 was added to 1 mL of 50 mM Tris-HCl buffer containing P(3HB) single crystals (0.4 mg/mL) in a transparent plastic cuvette and then incubated at 37 °C. The turbidity (mOD) at 660 nm (OD₆₆₀) was measured during enzymatic hydrolysis up to 90 min. To observe the time-dependent changes in the morphology of single crystals, 1 μ L of diisopropyl fluorophosphate was added into the reaction mixture at various reaction periods. The mixture was then centrifuged and washed twice with distilled water to remove the buffer. The crystals were then redispersed in ethanol, washed several times by centrifugation, and resuspended in ethanol.

Adsorption of PHB Depolymerase on Single Crystals. Adsorption of PHB depolymerase on P(3HB) single crystals was examined using an immuno-gold labeling technique. Antiserums against extracellular PHB depolymerases from *Comamonas acidovorans* YM1609 and *Alcaligenes faecalis* T1 were given by injecting 1 mg of PHB depolymerase mixed with the complete Freund's adjuvant into a mature white New Zealand rabbit. In the case of *C. acidovorans* YM1609, a booster injection of 0.3 mg of PHB depolymerase was applied in the same manner 66 days later. The antiserum titer was determined with Western-blotting method.³² The antiserum, 11 weeks later, was collected and stored at 4 °C. Anti-rabbit IgG (whole molecule) gold conjugate (10 nm nominal particle diameter) was obtained from Sigma Bio Sciences.

A 4 μ L sample of a 200 μ g/mL solution of extracellular PHB depolymerase was mixed with 1 mL of a 0.4 mg/mL suspension of P(3HB) single crystals in 50 mM Tris-HCl buffer (pH 7.5). The mixture was incubated at 37 °C for 5–60 min to allow adsorption of enzyme to the surface of single crystals. When required over 10 min for the adsorption of extracellular PHB depolymerases, 1 μ L of diisopropyl fluorophosphate was added into the reaction mixture to stop the enzymatic degradation. After the mixture was washed three times by centrifugation with DIG1 buffer containing 1% skim milk and 0.5 M NaCl (DIG1-SM-NaCl buffer), P(3HB) single crystals were resuspended in 1 mL of DIG1-SM-NaCl buffer, mixed with 10 μ L of antiserum against PHB depolymerase, and incubated at room temperature for 3 h. The P(3HB) single crystals were washed once with DIG1-SM-NaCl buffer, twice with DIG1 buffer containing only 0.5 M NaCl, and once with DIG1 buffer alone to remove unbonded antiserum against PHB depolymerase. The P(3HB) single crystals were resuspended in 200 μ L of DIG1 buffer, mixed with 10 μ L of anti-rabbit IgG gold conjugation, and incubated at room temperature for 30 min. Then, the gold-labeled preparation was washed three times with DIG1 buffer, and finally resuspended in 200 μ L of DIG1 buffer, for deposition on carbon-coated electron microscope grids.

Molecular Weight Measurement. All molecular weight data of P(3HB) single crystals before and after enzymatic degradation were obtained by gel-permeation chromatography (GPC) at 40 °C, using a Shimadzu 10A GPC system and 6A refractive index detector with joint columns of Shodex K-80M and K-802 (each 4.6 \times 300 mm). Chloroform was used as an eluent at a flow rate of 0.8 mL/min, and a sample concentration of 1.0 mg/mL was employed. The number-average and weight-average molecular weights (M_n and M_w) were calculated by using a Shimadzu Chromatopac C-R7A plus equipped with a GPC program. A molecular weight calibration curve of P(3HB) was obtained on the basis of the universal calibration method³³ with polystyrene standards of low polydispersities.

Transmission Electron Microscopy. Drops of P(3HB) crystals suspension, before and after enzymatic degradation, were deposited on carbon-coated grids, allowed to dry, and then shadowed with a Pt-Pd alloy. For electron diffraction pur-

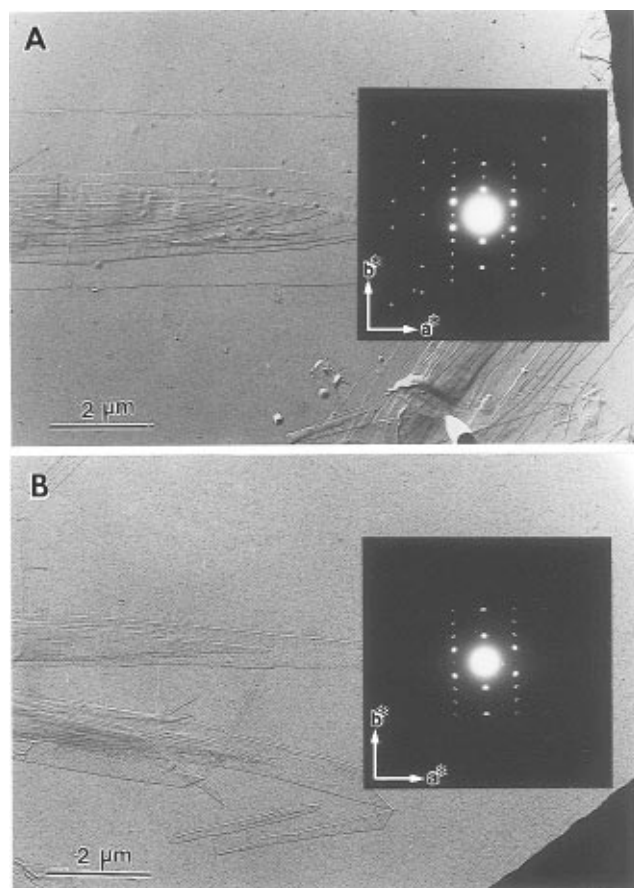


Figure 2. Electron micrographs of P(3HB) single crystals, (A) HMW-P(3HB) and (B) LMW-P(3HB), grown from a mixture of chloroform and ethanol, shadowed with a Pt–Pd alloy. Inset: typical electron diffraction pattern corresponding to a single crystal.

poses, the crystals were only allowed to dry. Small drops of P(3HB) crystals suspension, with and without gold labeling, were placed on carbon-coated grids, and then allowed to dry. These grids were observed with a JEM-2000FX II electron microscope operated at an acceleration voltage of 120 kV for both electron diffraction and imaging of shadowed crystals. Electron diffraction diagrams and images were recorded on Kodak SO-163 and 4489 films, respectively, developed for 4 min with Kodak D19 developer (diluted in water 1/2, v/v).

Atomic Force Microscopy. The thicknesses of P(3HB) single crystals, before and after enzymatic degradation, were investigated on the basis of atomic force microscopy (AFM). AFM was performed with a SPI3700/SPA300 (Seiko Instruments Inc.). Pyramid-like Si_3N_4 tips, mounted on 100 μm long micro cantilevers with spring constants of 0.09 N/m were applied for the contact mode experiments. Simultaneous registration was performed in the contact mode for height and deflection images. Drops of crystal suspension, before and after enzymatic degradation, were given on mica and allowed to dry. All images were recorded at room temperature.

Results and Discussion

Typical electron micrographs of single crystals of the two different molecular weights of P(3HB), HMW-P(3HB) ($M_n = 34\,000$ and $\text{DPI} = 2.6$) and LMW-P(3HB) ($M_n = 1700$ and $\text{DPI} = 1.2$), are shown in parts A and B of Figure 2, respectively. HMW-P(3HB) yields multilamellar lath-shaped crystals grown from the aggregation center, while LMW-P(3HB) gives as lath-shaped crystals with dimensions of around $0.3\text{--}1\ \mu\text{m}$ along the short and of around $5\text{--}10\ \mu\text{m}$ along the long axes. During their handling and especially during the centrifugation step, these crystals get broken as shown in Figure 2B. Each monolamellar part of both single

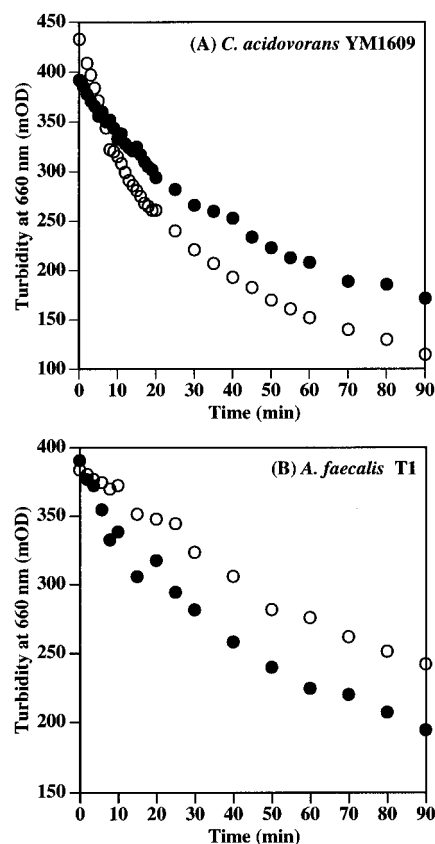


Figure 3. Decrease in turbidity versus time during the enzymatic degradation of (●) LMW-P(3HB) single crystals and (○) HMW-P(3HB) single crystals, with extracellular PHB depolymerases: (A) *C. acidovorans* YM1609 and (B) *A. faecalis* T1.

crystals yields a sharp electron diffraction pattern, and these are illustrated in parts A and B of Figure 2 as the inset diagrams. These diagrams are defined by the two orthogonal axes a^* and b^* , and systematic absences occur at every odd reflection along these two axes. Thus, these diffraction patterns are consistent with a p_{gg} symmetry. Furthermore, based on P(3HB) having an orthogonal crystal system,³⁴ the polymer chains align perpendicular to the lamellar base of the crystal. Resulting from the triple-exposure of the selected-area electron diffraction and the normal and selected-area images, it was confirmed that the long axes of both single crystals were their crystallographic a axes, as previously reported.^{22,30,35–37}

The thickness by AFM of the monolamellar part of both single crystals yielded values of around 5 nm, in spite of the difference in molecular weight. Sykes *et al.*³⁸ reported that the single crystals prepared from an oligomer of 32 HB units had 5 nm lamellar thickness and this oligomer folded once within a crystal. In the case of LMW-P(3HB) single crystals in this study, the degree of polymerization of P(3HB) chain in single crystals is about 20. Taking the fiber repeat distance of 0.596 nm with twofold screw symmetry along the molecular axis³⁴ into consideration, chain-folding at the lamellar surface may not occur in the LMW-P(3HB) single crystals. On the other hand, HMW-P(3HB) single crystals ($M_n = 34\,000$) should have the chain-folding surfaces.

Degradation by *C. acidovorans* YM1609 Depolymerase. The turbidimetric profiles for the degradation of LMW- and HMW-P(3HB) single crystals by an extracellular PHB depolymerase from *C. acidovorans* YM1609 is shown in Figure 3A. In our previous report using an extracellular PHB depolymerase isolated from

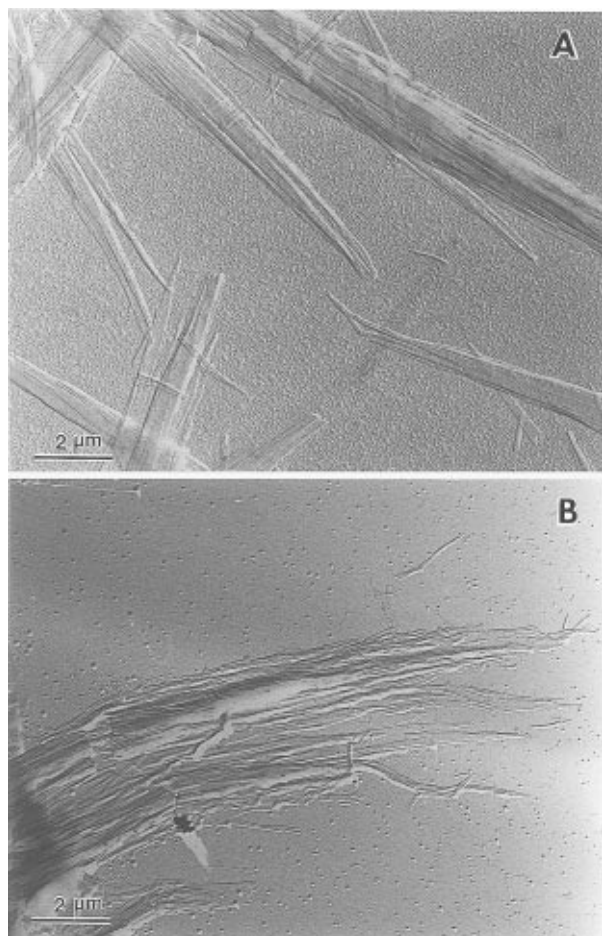


Figure 4. Electron micrographs of P(3HB) single crystals after enzymatic degradation by an extracellular PHB depolymerase purified from *C. acidovorans* YM1609: (A) LMW-P(3HB) single crystals after 40 min of enzymatic hydrolysis; (B) HMW-P(3HB) single crystals after 40 min of enzymatic hydrolysis.

P. stutzeri YM1006,³⁰ the turbidity decreased with time along two different lines which seemed to correspond to the degradations of the amorphous region of the crystal edges and surfaces and of the tight chain-packing crystal region, respectively, during the enzymatic hydrolysis. However, in this study the turbidity decreased without clear differences of the slopes, as in the case of degradation of P(3HB) single crystals using PHB depolymerases from the fungus *Aspergillus fumigatus* and the bacterium *P. lemoignei* reported by Hocking *et al.*²⁸

Typical electron micrographs of LMW- and HMW-P(3HB) single crystals after 40 min of enzymatic hydrolysis are shown in parts A and B of Figure 4, respectively. In spite of the differences in the surface morphologies, both single crystals were degraded to small crystal fragments with narrow cracks. The same behaviors have already been reported, by Nobes *et al.*,²⁹ for bacterial P(3HB) single crystals ($M_n = 174\,000$), in which chain-foldings existed on the crystal surfaces, degraded by *P. lemoignei* PHB depolymerase A. They found that single crystals splintered parallel to their long axes during the enzymatic degradation and confirmed that these crystals kept high crystallinity by electron diffraction. Our electron micrographs also showed that the single crystals were splintered along their long axes, resulting in the formation of the small crystal fragments by perpendicular attack to their long axes by enzyme. Noticeably, in the case of LMW-P(3HB) single crystals as shown in Figure 4A, the same

splintered crystals and fragments could be observed.

The molecular weights and polydispersities of HMW-P(3HB) single crystals remained unchanged before and after enzymatic degradation, indicating that the partial degradation at chain-folding surface does not take place. This result is consistent with our previous experiment using *P. stutzeri* YM1609 PHB depolymerase³⁰ and with the report by Hocking *et al.*²⁷ using enzymes from the fungus *A. fumigatus* and the bacterium *P. lemoignei*.

AFM images and line profile data of HMW-P(3HB) single crystals before and after enzymatic degradation are shown in Figure 5. The monolamellar part of crystals remained around 5 nm thickness, which was unchanged before and after enzymatic degradation. Both GPC and AFM data showed no evidence for the enzymatic degradation from crystal surface. In the case of LMW-P(3HB) single crystals, the thickness of monolamellar part remained unchanged during the enzymatic hydrolysis (data not shown).

Taking the chain-folding direction in P(3HB) crystals, confirmed by Birley *et al.*³⁵ using the polyethylene decoration method, into consideration, HMW-P(3HB) single crystals, which exist as successive folds in [110] and $[1\bar{1}0]$ directions, were degraded from untied chains of crystal ends (*bc* plane). Furthermore, taking the crystal growth mechanism of HMW-P(3HB) single crystals into consideration, the splintering and fragmentation of crystals takes place by the *endo-exo* type activity of PHB depolymerase. P(3HB) chains, connected by hydrogen bonding energy in the direction of crystal growth,³¹ are packed by weak van der Waals energy along the crystal width. Accordingly, the weak points (*e.g.* loosely packed region) attacked by *endo-exo* type enzymes should be located at the crystal edges (*ac* plane) and ends (*bc* plane), resulting in the formation of many narrow cracks and crystal fragments. In addition, the result on the degradation morphology of LMW-P(3HB) single crystals implies combined *endo-exo* enzyme activity.

LMW-P(3HB) single crystals have little chain-folding on the crystal surfaces. Every chain at the crystal edges and ends is energetically the same. In our previous report using an extracellular PHB depolymerase from *P. stutzeri* YM1609, as degradation time passed, the edges of LMW-P(3HB) single crystals became rough and the crystal size decreased without making cracks, which suggested that this enzyme operated with *exo*-type activity.³⁰ If the rate-determination step of enzymatic degradation by *C. acidovorans* YM1609 PHB depolymerase were that P(3HB) chains are untied from the crystal edges similar to the case of *P. stutzeri* YM1006 PHB depolymerase with predominant *exo*-type activity, the crystals would not splinter and fragment. Accordingly, on the basis of the observation results of LMW-P(3HB) single crystals, it may be concluded that the extracellular PHB depolymerase from *C. acidovorans* YM1609 has *endo*-type activity together with *exo*-type activity.

Degradation by *A. faecalis* T1 Depolymerase.

The turbidimetric degradation profiles for both single crystals by an extracellular PHB depolymerase from *A. faecalis* T1 is shown in Figure 3B. Typical electron micrographs of both single crystals after 80 min of enzymatic hydrolysis are shown in parts A and B of Figure 6, respectively. In spite of the differences in surface morphologies, as the case of *C. acidovorans* YM1609 described in the preceding section, both single crystals were degraded along the long axes of the crystals as making the narrow cracks and small crystal fragments. In addition, it was quite obvious that

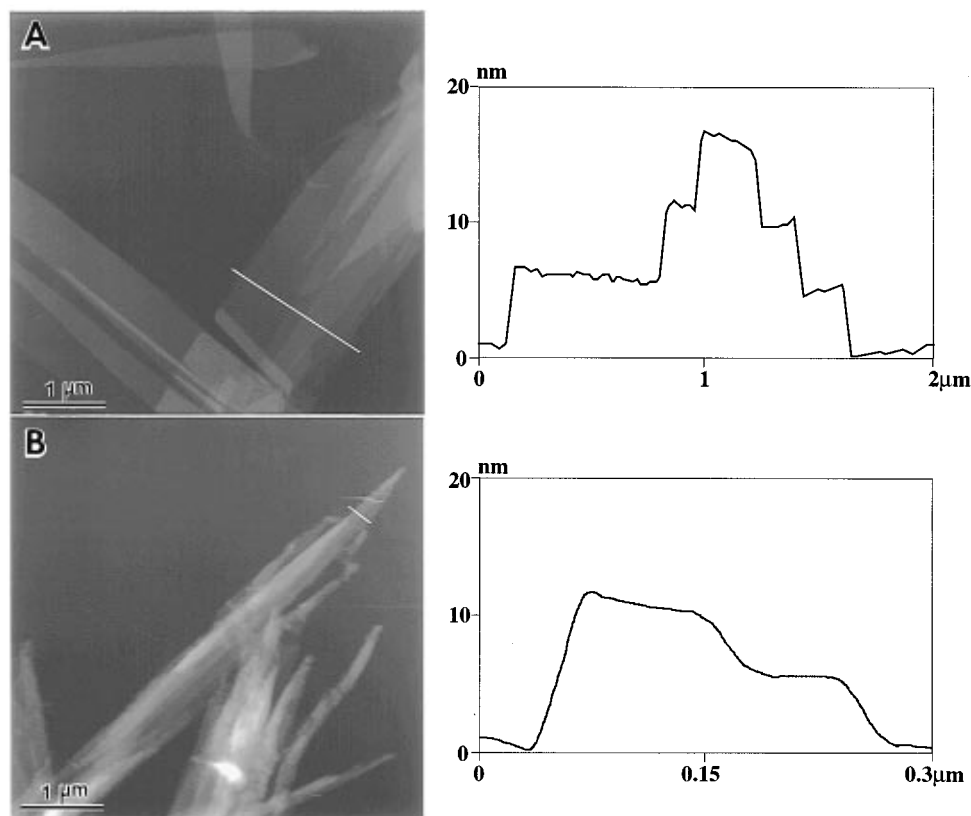


Figure 5. AFM images of HMW-P(3HB) single crystals and line profile data: (A) before and (B) after enzymatic degradation by an extracellular PHB depolymerase purified from *C. acidovorans* YM1609.

enzymatic attacks occurred from the both ends of the crystals. When the electron diffraction of the remaining crystals or crystal fragments was tested, the crystal gave a well-defined electron diffraction pattern. AFM measurements of both crystals before and after enzymatic degradation showed the almost same thicknesses of monolamellar parts (data not shown) which indicated the enzymatic degradation had not occurred to the direction of lamellar thickness (*c* axis). The molecular weights of single crystals remained unchanged before and after enzymatic degradation (data not shown), as the cases of PHB depolymerases from *C. acidovorans* YM1609, *P. stutzeri* YM1006³⁰ and *P. lemoignei*.²⁸

All results of crystal morphologies, lamellar thicknesses and molecular weights indicated that *A. faecalis* T1 PHB depolymerase defined as type I and *C. acidovorans* YM1609 PHB depolymerase as type II had the same manner of enzymatic activity with *endo-exo* behavior. Thus, the difference in the position of the lipase box in the catalytic domain of enzyme might have little effect on the degradation manner of crystal region. Furthermore, considering the results with *P. lemoignei* PHB depolymerase A defined as type III, which has threonine-rich region as the linker domain, having also *endo-exo* combined activity,²⁹ it should be concluded that PHB depolymerases have the same degradation mechanism in spite of the difference in the structure of enzymes.

Adsorption of PHB Depolymerases. Visualizations of the adsorption of extracellular PHB depolymerases purified from *C. acidovorans* YM1609 and *A. faecalis* T1 to HMW-P(3HB) single crystals, which have chain-folding surfaces, by using anti-rabbit IgG gold conjugation are shown in parts A and B of Figure 7, respectively. Homogeneous distributions of extracellular PHB depolymerases on the surface of single crystals were observed for both the type II, *C. acidovorans* YM1609, PHB depolymerase and the type I, *A. faecalis*

T1, PHB depolymerase. In spite of the homogeneous distribution of extracellular PHB depolymerase on crystal surfaces, the enzymatic degradation took place at crystal edges and ends rather than the chain-folding surfaces. This phenomenon should be explained by the steric hindrance of methyl group or the difference of the conformation between P(3HB) residues.

On the other hand, the adsorption of two kinds of extracellular PHB depolymerases to LMW-P(3HB) single crystals, which have little chain-folding surface, are shown in Figure 8. The typical electron micrograph of single crystals adsorbed by *C. acidovorans* YM1609 PHB depolymerase shows a slightly higher concentration of enzyme at the ends of crystals in Figure 8A. Furthermore, an uniform distribution is detected along the long axes of the crystals. Figure 8B shows the image of the adsorption of *A. faecalis* T1 PHB depolymerase, which is consistent with that observed with *C. acidovorans* YM1609 PHB depolymerase.

For both enzymes the adsorption to LMW-P(3HB) crystals was weaker than that to HMW-P(3HB) crystals. This phenomenon might be in terms of the following adsorption mechanism of extracellular PHB depolymerases. Enzyme molecules cannot bind strongly to the surface of LMW-P(3HB) crystals by hydrophobic adsorption since P(3HB) chain ends with hydroxyl and carboxyl groups are waving on the surface. Furthermore, for these enzymes to adhere with multipoint adsorptions to P(3HB) chains of crystal surfaces and edges, regular surface morphology may be required. HMW-P(3HB) single crystals have a regular folded-chain crystal surface, while LMW-P(3HB) crystal surfaces are rougher than those of HMW-P(3HB), based on the results of AFM data. As the results, enzymes bind much more and bind stronger to the HMW crystal surface.

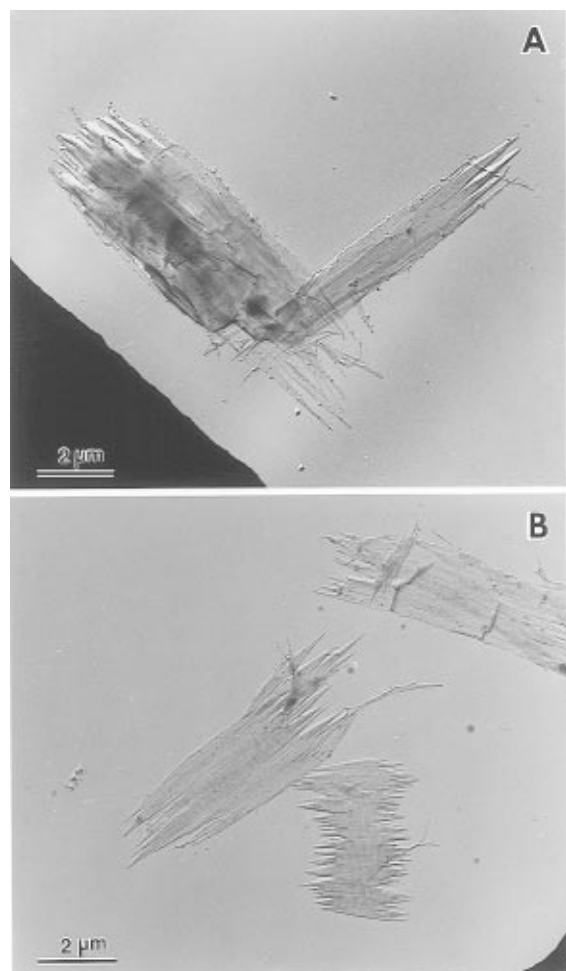


Figure 6. Electron micrographs of P(3HB) single crystals after enzymatic degradation by an extracellular PHB depolymerase purified from *A. faecalis* T1: (A) LMW-P(3HB) single crystals after 80 min of enzymatic hydrolysis; (B) HMW-P(3HB) single crystals after 80 min of enzymatic hydrolysis.

Until now, the specificity for the binding-domain of extracellular PHB depolymerase to the surface of some polyhydroxyalkanoates (PHA), poly(4-hydroxybutyrate), poly(3-hydroxyvalerate) and etc., or P(3HB) films with different stereoregularities has been investigated. Kasuya *et al.* concluded that the binding domain of PHB depolymerase purified from *A. faecalis* T1 was non-specific for the binding to the surface of PHA films based on the values of adsorption equilibrium constant.³⁹ Furthermore, Abe and Doi reported that the rate of adsorption of same PHB depolymerase was dependent in the stereochemical structure of P(3HB) chains on the surface of film.⁴⁰ They also concluded that enzymatic degradation occurred by the two steps of adsorption and hydrolysis where the first step was an adsorption by the binding domain and the second step was a hydrolysis by the catalytic domain based on the kinetic data. Taking these results into consideration, the majority of PHB depolymerase molecules adsorbed on the surface could contribute to an increase in the mobility of P(3HB) chains as a whole.

The active sites of enzyme might not be able to attack the regular sharp folds and chains in the crystals directly, and hydrophobic binding of PHB depolymerase might be required to create the disordered regions in the crystals. In addition, the P(3HB) chains at the crystal edges are more mobile than those in the crystal from the point of view of the chain packing, resulting in the degradation of P(3HB) chains from the crystal edges. The chains untied from the crystal edges by the

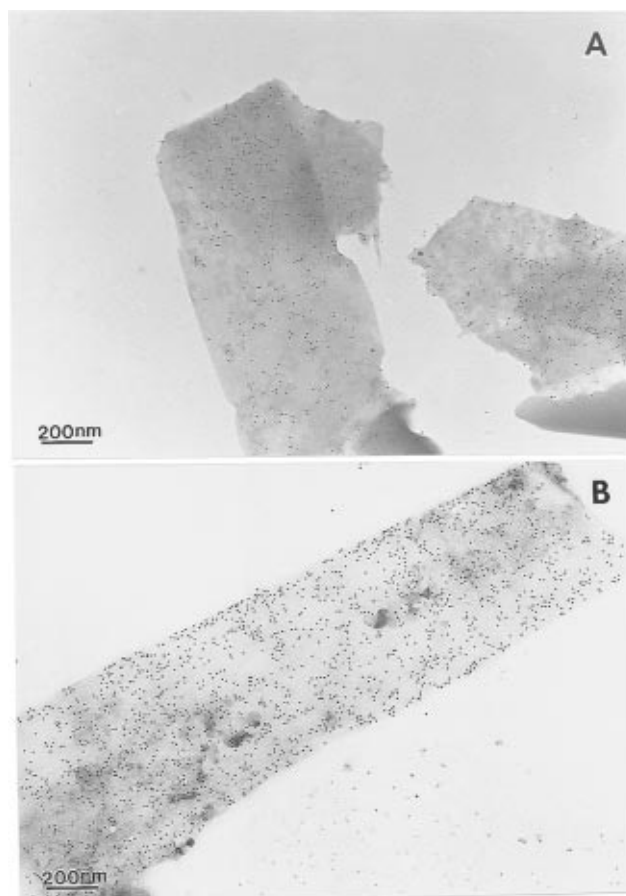


Figure 7. Visualization of the adsorption of two kinds of extracellular PHB depolymerases to HMW-P(3HB) single crystals, (A) *C. acidovorans* YM1609 and (B) *A. faecalis* T1, by gold labeling and transmission electron microscopy.

adsorption or chains being cut off by *endo*-type activity are likely be degraded by *exo*-type enzyme activity.

Recently, Harjunpää *et al.* described the processive degradation as the hydrolysis of soluble cello-oligosaccharides catalyzed by cellobiohydrolase II, and they concluded that this processivity should be a principal importance for the degradation of cellulose.⁴¹ Furthermore, Braun *et al.* proposed a processive degradation as one of the degradation mechanism of polymers by poly(ADP-ribose) glycohydrolase; *i.e.* endoglycosidic cleavage plus exoglycosidic.⁴² If this concept could be applied to extracellular PHB depolymerase, the hydrolysis by *endo-exo* enzymatic behavior might be described as processive degradation.

Conclusions

This paper has reported the visualization of enzymatic degradation of P(3HB) single crystals having different surface morphologies with extracellular PHB depolymerases from *A. faecalis* T1 and *C. acidovorans* YM1609 defined as types I and II, respectively. Enzymatic degradation of single crystals by both PHB depolymerases progressed from the edges and along their long axis rather than the chain-folding surfaces yielding the narrow cracks and crystal fragment. Adsorption of PHB depolymerase to single crystals was studied using an immuno-gold labeling technique, which demonstrated a homogeneous distribution of enzyme molecules on the chain-folding surfaces of HMW-P(3HB) crystals. However, a relatively high concentration of enzyme was observed on the edges and ends of LMW-P(3HB) crystals, rather than on the no-chain-folding surface.

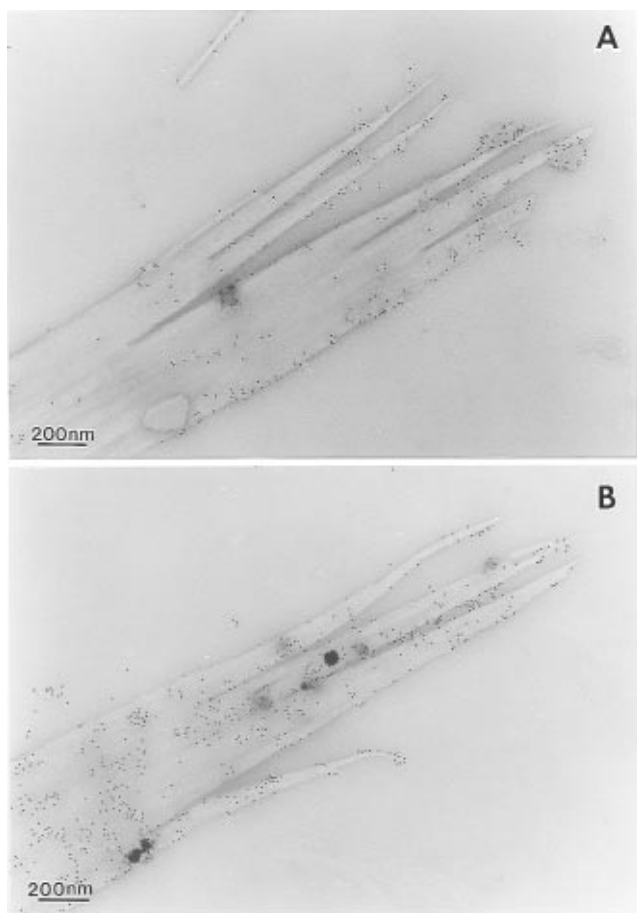


Figure 8. Visualization of the adsorption of two kinds of extracellular PHB depolymerases to LMW-P(3HB) single crystals, (A) with *C. acidovorans* YM1609 PHB depolymerase and (B) with *A. faecalis* T1 PHB depolymerase, by gold labeling and transmission electron microscopy.

On the basis of these results, it has been concluded that the adsorption of PHB depolymerase on the single crystals has a great effect to increase the mobility of P(3HB) chains in crystals, and that the *exo*-type attack by the active site of PHB depolymerase takes place preferentially against the chain-packing region disordered by *endo*-type activity or adsorption of enzyme. Thus, P(3HB) chains are untied from the crystal edge or cropped out from the crystals, rather than the chain-folding surfaces of single crystals, and hydrolyzed by the enzyme with *endo-exo* behavior. Furthermore, it has been demonstrated that the two extracellular PHB depolymerases have the same enzymatic degradation manner and adsorption mechanism, in spite of the difference in the structure of the enzymes.

Acknowledgment. This work has been supported by CREST (Core Research for Evolutional Science and Technology) of Japan Science and Technology Corporation (JST).

References and Notes

- (1) Dawes, E. A.; Senior, P. J. *Adv. Microbiol. Physiol.* **1973**, *10*, 135.
- (2) Anderson, A. J.; Dewes, E. A. *Microbiol. Rev.* **1990**, *54*, 450.
- (3) Doi, Y. *Microbial Polyesters*; VCH Publishers: New York, 1990.
- (4) Lusty, C. J.; Doudoroff, M. *Proc. Natl. Acad. Sci. U.S.A.* **1966**, *56*, 960.
- (5) Tanio, T.; Fukui, T.; Shirakura, Y.; Saito, T.; Tomita, K.; Kaiho, T.; Masamune, S. *Eur. J. Biochem.* **1982**, *124*, 71.
- (6) Mukai, K.; Yamada, K.; Doi, Y. *Polym. Degrad. Stab.* **1993**, *41*, 85.
- (7) Mukai, K.; Yamada, K.; Doi, Y. *Polym. Degrad. Stab.* **1994**, *43*, 319.
- (8) Yamada, K.; Mukai, K.; Doi, Y. *Int. J. Biol. Macromol.* **1993**, *15*, 215.
- (9) Kasuya, K.; Inoue, Y.; Tanaka, T.; Akehata, T.; Iwata, T.; Fukui, T.; Doi, Y. Submitted to *Appl. Environ. Microbiol.*
- (10) Saito, T.; Suzuki, K.; Yamamoto, J.; Fukui, T.; Miwa, K.; Tomita, K.; Nakanishi, S.; Odani, S.; Suzuki, J.; Ishikawa, K. *J. Bacteriol.* **1989**, *171*, 184.
- (11) Müller, B.; Jendrossek, D. *Appl. Microbiol. Biotechnol.* **1993**, *38*, 487.
- (12) Gilkes, N. R.; Henrissat, B.; Kiburn, D. G.; Miller, R. C.; Warren, R. A. J. *Microbiol. Rev.* **1991**, *55*, 303.
- (13) Wong, K. K. Y.; Tan, L. U. L.; Saddler, J. N. *Microbiol. Rev.* **1992**, *52*, 305.
- (14) Kellet, L. E.; Poole, D. M.; Ferreira, L. M. A.; Durrant, A. J.; Hazlewood, G. P.; Gilbert, H. J. *Biochem. J.* **1990**, *272*, 369.
- (15) Watanabe, T.; Suzuki, K.; Oyanagi, W.; Ohnishi, K.; Tanaka, H. *J. Biol. Chem.* **1990**, *265*, 15659.
- (16) Robbins, P. W.; Overbye, K.; Albright, C.; Benfield, B.; Pero, J. *Gene* **1992**, *111*, 69.
- (17) Jendrossek, D.; Backhaus, M.; Andermann, M. *Can. J. Microbiol.* **1995**, *41* (Suppl. 1), 160.
- (18) Klingbeil, B.; Kroppenstedt, R. M.; Jendrossek, D. *FEMS Microbiol. Lett.* **1996**, *142*, 215.
- (19) Jendrossek, D.; Frisse, A.; Behrends, A.; Andermann, M.; Kratzin, H. D.; Stanislawski, T.; Schlegel, H. G. *J. Bacteriol.* **1995**, *177*, 596.
- (20) Shiraki, M.; Shimada, T.; Tatsumichi, M.; Saito, T. *J. Environ. Polym. Degrad.* **1995**, *3*, 13.
- (21) Doi, Y.; Kitamura, S.; Abe, H. *Macromolecules* **1995**, *28*, 4822.
- (22) Kumagai, Y.; Kanesawa, Y.; Doi, Y. *Makromol. Chem.* **1992**, *193*, 53.
- (23) Tomasi, G.; Scandola, M.; Briese, B. H.; Jendrossek, D. *Macromolecules* **1996**, *29*, 507.
- (24) Koyama, N.; Doi, Y. *Macromolecules* **1997**, *30*, 826.
- (25) Chanzy, H.; Comtat, J.; Dube, M.; Marchessault, R. H. *Biopolymers* **1979**, *18*, 2459.
- (26) Marchessault, R. H.; Revol, J.-F.; Bobbitt, T. F.; Hordin, J. H. *Biopolymers* **1980**, *19*, 1069.
- (27) Hocking, P. J.; Revol, J.-F.; Marchessault, R. H. *Macromolecules* **1996**, *29*, 2467.
- (28) Hocking, P. J.; Marchessault, R. H.; Timmins, M. R.; Lenz, R. W.; Fuller, R. C. *Macromolecules* **1996**, *29*, 2472.
- (29) Nobes, G. A. R.; Marchessault, R. H.; Chanzy, H.; Briese, B. H.; Jendrossek, D. *Macromolecules* **1996**, *29*, 8330.
- (30) Iwata, T.; Doi, Y.; Kasuya, K.; Inoue, Y. *Macromolecules* **1997**, *30*, 833.
- (31) Marchessault, R. H.; Coulombe, S.; Morikawa, H.; Okamura, K.; Revol, J.-F. *Can. J. Chem.* **1981**, *59*, 38.
- (32) Towbin, H.; Staehelin, T.; Gordon, J. *Proc. Natl. Acad. Sci. U.S.A.* **1979**, *76*, 4350.
- (33) Grubisic, Z.; Rempp, R.; Benoit, H. *J. Polym. Sci., Part B* **1967**, *5*, 753.
- (34) Yokouchi, M.; Chatani, Y.; Tadokoro, H.; Teranishi, K.; Tani, H. *Polymer* **1973**, *14*, 267.
- (35) Birley, C.; Briddon, J.; Sykes, K. E.; Barker, P. A.; Organ, S. J.; Barham, P. J. *J. Mater. Sci.* **1995**, *30*, 633.
- (36) Revol, J.-F.; Chanzy, H. D.; Deslandes, Y.; Marchessault, R. H. *Polymer* **1989**, *30*, 1973.
- (37) Deslandes, Y.; Orts, W.; Sundararajan, P. R.; Marchessault, R. H.; Revol, J.-F.; Chanzy, H. D. *Polym. Prepr. (Am. Chem. Soc., Div. Polym. Chem.)* **1989**, *29*, 607.
- (38) Sykes, K. E.; McMaster, T. J.; Miles, M. J.; Barker, P. A.; Barham, P. J.; Seebach, D.; Müller, H.-M.; Lengweiler, U. D. *J. Mater. Sci.* **1995**, *30*, 623.
- (39) Kasuya, K.; Inoue, Y.; Doi, Y. *Int. J. Biol. Macromol.* **1996**, *19*, 35.
- (40) Abe, H.; Doi, Y. *Macromolecules* **1996**, *29*, 8683.
- (41) Harjunpää, V.; Telemann, A.; Koivula, A.; Ruohonen, L.; Teeri, T.; Telemann, O.; Drakenberg, T. *Eur. J. Biochem.* **1996**, *240*, 584.
- (42) Braun, S. A.; Panzeter, P. L.; Collinge, M. A.; Althaus, F. R. *Eur. J. Biochem.* **1994**, *220*, 369.

MA970491G